ISSN: 2395-7852

# International Journal of Advanced Research in Arts, Science, Engineering & Management (IJARASEM )

Volume 11, Issue 3, May-June 2024

INTERNATIONAL STANDARD SERIAL NUMBER INDIA

IMPACT FACTOR: 7.583

| www.ijarasem.com | ijarasem@gmail.com | +91-9940572462 |

International Journal of Advanced Research in Arts, Science, Engineering & Management (IJARASEM)

| ISSN: 2395-7852 | www.ijarasem.com | Impact Factor: 7.583 | Bimonthly, Peer Reviewed & Referred Journal|

| Volume 11, Issue 3, May-June 2024 |

# Exploring the Magnetic Properties of Nanoparticles: Synthesis, Characterization and Applications

**Anil Kumar**

Assistant Professor, Department of Physics, Govt. Bangur College, Didwana, Rajasthan, India

**ABSTRACT:** The physical properties of magnetic nanoparticles are strongly influenced by their size. As the particle size decreases to the nanoscale, quantum effects become more prominent, leading to distinct phenomena like size-dependent magnetic behavior and enhanced surface-to-volume ratio.

**KEYWORDS:** nanoparticles, magnetic, synthesis, characterization, applications

## I. INTRODUCTION

Magnetic properties of nanoparticles are used for drug delivery, therapeutic treatment, contrast agents for MRI imaging, bioseparation, and in-vitro diagnostics. These nanometer-sized particles are superparamagnetic, a property resulting from their tiny size—only a few nanometers—a fraction of the width of a human hair (nanoparticles are approximately 1/1,000 thinner than human hair). Superparamagnetic nanoparticles are not magnetic when located in a zero magnetic field, but they quickly become magnetized when an external magnetic field is applied. When returned to a zero magnetic field they quickly revert to a non-magnetized state. Superparamagnatism is one of the most important properties of nanoparticles used for biomagnetic separation.

How nanoparticles are made

Magnetic nanoparticles are usually based on magnetite and/or maghemite, two different forms of iron oxide. The most popular way of obtained it is co-precipitation, where the material is directly synthesized as spherical particles. Controlling the synthesis parameters, it is possible to achieve sizes of less of 10 nm. Researchers and industrials are continuously improving the chemical or physical methods to achieve a better control of both composition (ratio magnetite/maghemite) and size and thus, the magnetic properties.

Applications of nanoparticles

Individually or as composites, the unique features of nanoparticles allow them to be used for a variety of applications:

- Carriers: Nanoparticles can be used to deliver molecules to targeted locations. This can be for the purpose of diagnosis or for drug delivery.
- Biomedical devices: Innovators in the biomedical field are using nanoparticles for diagnostic array development. When combined with fluorescent tagging technology the particles are also used for imaging. [1,2,3]
- Food safety: Nanoparticles have been used for creating packaging for better food preservation and for more targeted use of pesticides in food growth.
- Biomedical research: nanoparticles of the magnetic variety are commonly used laboratories for magnetic separation of molecules.

Advantages of nanoparticles

Nanoparticles hold many advantages in their various uses. The particles have a large surface to volume ratio, making them efficient for use across disciplines. They can be made soluble in water, and not toxic to the body for effective use as a carrier in the human body. With externally applied stimuli, magnetic nanoparticles hold great power for targeting, imaging and separation of molecules. Magnetic nanoparticles can host a multitude of surface conditions while reacting to outside stimuli very precisely.

Magnetization of superparamagnetic properties of nanoparticles

Magnetization is defined as the extent to which a material becomes magnetized when placed within a magnetic field, and is a measure of the net magnetic dipole moment per unit volume. The magnetization is directly related to the applied magnetic field.

Magnetic susceptibility (χ) is a dimensionless quantity that indicates the degree of magnetization of a material in response to a magnetic field. Magnetic susceptibility is equal to the ratio of magnetic dipole moment to magnetic field.

- M=magnetization (magnetic dipole moment per unit volume)
- B=applied magnetic field
- χ=magnetic susceptibility

$\chi = M/B$

Non-magnetic materials, like water, are diamagnetic and experience a small negative response to the magnetic field. In the case of diamagnetic materials, the susceptibility is negative and has a value around -10e-5. Paramagnetic materials, like oxygen molecules, experience a slightly positive response to the magnetic field. In the case of paramagnetic materials, the magnetic susceptibility is around 10e-4 or 10e-5. In both cases, the magnetic dipoles attempt to align with the external magnetic field, and fight against thermal agitation. Diamagnetic and paramagnetic dipoles don't interact with each other, and their susceptibility at room temperature is very small.

The situation is very different for magnetic materials, which are technically defined as ferro and ferrimagnetic materials. In magnetic materials, each dipole interacts with its nearest neighbors. This inter-dipole interaction creates a high magnetic response throughout the material, with susceptibilities that can reach values higher than 10e3. The drawback is that the materials show magnetic hysteresis: after applying a magnetic field, the material will have 'memory', meaning that when the applied field returns to zero the material remains at a certain magnetization.
This is a very useful property for developing permanent magnets, but it is a problem for many Life Science applications. Ferromagnetic beads will remain magnetized after the removal of an applied magnetic field, and the beads will form irreversible clumps or aggregates. The ideal material for biological applications would have a high magnetic susceptibility, but no magnetic 'memory'. They would combine a high response to applied magnetic field with a non-magnetic behavior once the magnetic field is removed.

Advances in nanotechnology have provided a way to obtain these superparamagnetic properties of nanoparticles by reducing the size of the ferro- or ferrimagnetic material to few nanometers (below the so-called superparamagnetic diameter). When they are below the superparamagnetic diameter the nanoparticles are able to return quickly to a non-magnetized state after an external magnet is removed. Larger ferro- and ferrimagnetic materials have remnant magnetism after the applied magnetic field returns to zero.

Now that you have learned all about the magnetic nanoparticle technology, let us discuss in more detail how they are used. For example, magnetic nanoparticles can be used to purify antibodies from a mixture in solution. These magnetic nanoparticles are pre-conjugated to a molecule that specifically binds antibodies, or immunoglobulins. These types of molecules are called either "protein A" or "protein G", as well as a hybrid called "protein A/G". You choose which one you use based on the subclass of antibody you are interested in purifying and from which organism it comes from.

Once the antibodies bind to the magnetic particles, also called magnetic beads, you can change out the liquid in the container by placing it in a magnetic rack. A magnetic rack will keep the magnetic particle bound to your antibodies in place, while the liquid can be removed. You can wash the particles while they are bound by the magnetic rack. Lastly you can elute the antibodies from the beads.

One of the limitations of this technique in the past was the size of the magnetic rack that is available. Magnetic racks are now available in a large variety of sizes from milliliter to tens of liters in size. This makes the technique useful from a laboratory scale to the scale of industry.

## II. DISCUSSION

Among hard/soft nanocomposites (NCs), ferrite-based materials are potentially promising for developing exchange-coupled systems, thus leading to enhanced magnetic properties. In this regard, we investigate the role of the synthesis approach in the development of $SrFe_{12}O_{19}/CoFe_2O_4$ (SFO/CFO) NCs, with special focus on tuning the magnetic features of the softer phase (CFO) by introducing $Zn^{2+}$ in the spinel structure. X-ray powder diffraction (XRPD), transmission electron microscopy (TEM) and squid magnetometry were employed to clarify the relationship between morphology, size, and magnetic properties of the NCs, pointing out the feasibility of this method in obtaining successfully exchange-coupled systems.[4,5,6] This work shows how optimizing the intrinsic magnetic properties of the CFO may be used to tune the extrinsic ones of the NCs. Despite the promising results in magnetic coupling, our study clearly confirms/strengthens that an enhancement of remanent magnetization is the most important factor for improving the magnetic performance.

The design of hard/soft bi-magnetic nanocomposites (NCs) have gained increasing attention in recent years and challenged the scientific community. Indeed, these systems offer the possibility of widely tuning their magnetic properties (i.e. magnetic anisotropy, saturation magnetization) at the nanoscale [1], [2], as they are composed of two different ferro- or ferrimagnetic phases, with different extrinsic magnetic properties: a hard phase, with a high coercivity ($H_C$), and a soft one, with both a high saturation and remanent magnetization ($M_S$ and $M_R$) [3]. If exchange-coupling interaction occurs, such a combination shall result in a material with both enhanced coercivity and magnetization, thus leading to improved energy products $(BH)_{MAX}$. This quantity describes the maximum amount of magnetic energy that can be stored in a magnet [4], [5]. In fact, the novel magnetic interaction among the two phases at the interface may promote a significant enhancement of the remanence of the NC with only a small deterioration of the coercivity due to the introduction of a soft phase [1], [6]. To achieve this goal, it is essential to tightly control the morpho-structural features of both the phases and maximize their interfacial contact. In this regard, ferrite-based composites have shown to be promising in the field of permanent magnets (PMs), especially M−type $SrFe_{12}O_{19}$/spinel $MFe_2O_4$ (M: Co, Zn, Ni, Mn), owing to the potential magnetic performance (energy products of 40–460 kJ $m^{-3}$) of the hexagonal ferrite and the flexible crystal structure of the spinel ferrite, offering many possibilities to modulate the magnetic anisotropy and saturation magnetization [7], [8], [9], [10], [11]. Nevertheless, the lack of comprehensive studies in literature on the degree of magnetic coupling in such systems is rather limited, thus leading to the need of thoroughly investigating the complex magnetic interactions bringing it forth. Various studies on ferrite-based NCs are reported in literature, dealing mainly with composites prepared as powders by physical mixing of the two phases or different chemical one-pot synthesis [11], [12], [13], which clearly show the challenges in obtaining an efficient exchange-coupling related to the synthetic approach. In our recent studies, we have addressed the role of synthesis strategy in controlling the magnetic coupling in bi-magnetic composites, thus showing that is possible to use sol–gel technique as an easy, scalable, low-cost and green synthesis method to produce tightly coupled NCs [14], [15], [16], [17], [18]. In this work, we first have explored a possible way to modify the extrinsic magnetic properties at the nanoscale of a hard $SrFe_{12}O_{19}$ (SFO) phase (anisotropy constant K = 0.35 MJ/$m^3$, $M_S$ ~ 0.38 MA/m) introducing a softer $CoFe_2O_4$ (CFO) phase with a higher bulk $M_S$ ~ 0.45 MA/m and lower anisotropy (K = 0.29 MJ/$m^3$) [5], [19]. We use SFO/CFO 80/20 w/w % as the parent material and show the feasibility of introducing $Zn^{2+}$ cations into the spinel structure of CFO using the above mentioned one-pot synthesis method. Zinc was chosen to increase the softness of the spinel CFO, lowering $H_C$ and increasing $M_S$ by substituting $Co^{2+}$ with $Zn^{2+}$ [7], [20]. The effect of $Zn^{2+}$ substitution on the extrinsic properties of the exchange-coupled NC is investigated. Our goal is to optimize the magnetic properties of such NCs by atomic structuring and modification of the intrinsic characteristics of CFO [21], and prove the feasibility of the one-pot synthesis method to design and obtain strongly coupled NCs with an overall good control on the crystallite sizes and homogeneous distribution even in the presence of an additional dopant (Zn). Therefore, we prepared three different NCs by substituting $Co^{2+}$ in $Co_{1-x}Zn_xFe_2O_4$ with an increasing amount of $Zn^{2+}$ (with x = 0.1, 0.3, 0.5, nominally): indeed, spinel ferriteś versatile crystal structure offers many possibilities to modulate the magnetic anisotropy, due to the rearrangement of cationic distribution among the tetrahedral ($T_d$) and Octahedral ($O_h$) sites, by chemical engineering [20], [22], [23]. Our study reveals that optimizing the magnetic properties of each single component of the NC is fundamental to achieve exchange coupled nanostructures with enhanced magnetic performances.[7,8,9] It is important to note here that the change in $H_C$ of the NCs can be a direct result of the Zn-doping and hence, an intrinsic effect on the anisotropy of CFO, but it can also have extrinsic contributions like the coupling between the two phases and the resulting change in the reversal process.

To prepare various hard/soft SFO/CFO nanocomposites (NCs), with composition 80/20 w/w %, a one-pot sol–gel route was used, described elsewhere [18], [24]: briefly, two separate sols were first prepared by dissolving the precursors of SFO i.e., $Fe(NO_3)_3{\cdot}9H_2O$ and $Sr(NO_3)_2$ (Sigma-Aldrich) in a $[Fe^{3+}]/[Sr^{2+}]$ ratio of 11 (note that the initial non-stoichiometric starting ratio between Fe and Sr with a slightly higher presence of Sr enables the formation of SFO at lower temperatures [18]), and the precursors of CFO i.e., $Co(NO_3)_2{\cdot}6H_2O$ and $Fe(NO_3)_3{\cdot}9H_2O$ (Sigma-Aldrich) in a $[Fe^{3+}]/[Co^{2+}]$ ratio of 2 in deionized water Then a 1 M citric acid aqueous solution was added (molar ratio of total metals to citric acid 1:1), the dispersions were mixed together and the pH was adjusted to 7 by adding dropwise $NH_3$ (30%) (Sigma-Aldrich). Next, it was heated on a hot plate to 80 °C to form a dry gel, and the temperature was increased to 300 °C inducing a self-combustion. The obtained dry powders were ground and annealed at 950 °C for 3 h in air. We refer to this sample as NC. To evaluate the effect of magnetic anisotropy, three $SrFe_{12}O_{19}/Co_{1-x}Zn_xFe_2O_4$ ($NC_s$_Zn) samples were synthesized through this one-pot approach, using the same procedure as NC, however by substituting $Co^{2+}$ with $Zn^{2+}$(keeping constant $Fe^{3+}$) with x: 0.1–0.3–0.5. We refer to these in the rest of the article as NC_Zn01, NC_Zn03, and NC_Zn05.

The final composition was confirmed by means of inductively coupled plasma optical emission spectroscopy (ICP–OES), carried out for elemental analysis with an iCAP 6300 DUP ICP–OES spectrometer (ThermoScientific) (see Table 1). A first check to verify the presence of organic molecules (residuals from the gel) on the final samples was done by means of Fourier-transform infrared spectroscopy (FTIR): the spectra were acquired with a Shimadzu IRPrestige-21, equipped with a Specac Golden Gate Single Reflection Diamond Attenuated total reflection (ATR). All samples were analyzed in the region between 4000 $cm^{-1}$ and 400 $cm^{-1}$.

Table 1. List of samples, nominal composition and x: Zn content obtained from ICP analysis.

| Id | Composition (80/20 (w/w %)) | x ICP ($Co_{1-x}Zn_xFe_2O_4$) | Synthesis Method |
|---|---|---|---|
| NC | $SrFe_{12}O_{19}/CoFe_2O_4$ | – | One pot sol–gel |
| NC_Zn01 | $SrFe_{12}O_{19}/Co_{0.9}Zn_{0.1}Fe_2O_4$ | 0.11 | |
| NC_Zn03 | $SrFe_{12}O_{19}/Co_{0.7}Zn_{0.3}Fe_2O_4$ | 0.31 | |
| NC_Zn05 | $SrFe_{12}O_{19}/Co_{0.5}Zn_{0.5}Fe_2O_4$ | 0.53 | |

The powder samples were characterized using a Bruker D8 Advance diffractometer (solid state rapid LynxEye detector, Cu Kα radiation, Bragg–Brentano geometry, DIFFRACT plus software) in the 10°–140° 2θ range with a step size of 0.013° (counting time was 4 s per step). Rietveld analysis was performed on the X-ray powder diffraction (XRPD) data using the FULLPROF program [25]. The diffraction peaks were described by a modified Thompson-Cox-Hastings pseudo-Voigt function. A peak asymmetry correction was made for angles below 40° (2θ). Background intensities were estimated by interpolating between up to 60 selected points. A NIST $LaB_6$ 660b standard was measured under the same conditions as the samples to account for the instrumental contribution to the peak broadening.

Transmission electron microscopy (TEM) analysis was carried out using a Philips CM200 microscope operating at 200 kV and equipped with a $LaB_6$ filament. For TEM observations, the samples, in form of powder, were prepared using the following procedure. A small quantity of powder was dispersed in ethanol and subjected to ultrasonic agitation for approximately one minute. A drop of the suspension was deposited on a commercial TEM grid covered with a thin carbon film. Finally, the grid was kept in air until complete ethanol evaporation.

Magnetic measurements were performed at room temperature using a Quantum Design superconducting quantum interference device (SQUID) magnetometer, which can supply a maximum field of 5 T. Iso-thermal field-dependent magnetization loops were recorded by sweeping the field in the − 5 T to + 5 T range. To get information about the irreversible processes, direct current demagnetization (DCD) remanence curves were measured by applying a progressively higher DC reverse field to a sample previously saturated under a field of −5T and by recording, for each step, the value of the remanent magnetization, which was then plotted as a function of the reverse field [26]. To avoid any displacement and preferential orientation of the crystallites under the external magnetic field during measurement, the nanopowders were immobilized with a glue in appropriate capsules (no significant magnetic contribution from the glue was observed during the measurements).

## III. RESULTS

Magnetic nanoparticles (MNPs) have been extensively studied over the last half century and continue to sustain interest due to their potential use in fields ranging from high-density data storage [1] to biomedical applications [2,3]. The unique properties of MNPs derive from the fact that these nanoscale magnets differ from bulk materials due to their high surface-to-volume ratios. Owing to strong interest in their possible applications, several reviews of MNPs have been published [2,4], including those that focus on sensing [1,5], drug delivery [6–8], and hyperthermia [9]. Although there is a plethora of published information, a review that emphasizes the optimization of MNP properties to effectively target specific applications is lacking. The motivation for assembling this report was to provide a matrix of parameters to modulate and tune the properties of MNPs for a particular end-use. Recently, there has been substantial progress in the synthesis of MNPs of varying sizes, shapes, compositions, and shell-core designs [10,11]. This review will target the different factors that contribute to the control and optimization of the key magnetic properties of MNPs: saturation magnetization (Ms), coercivity (Hc), blocking temperature ($T_B$), and relaxation time ($t_N$ and $t_B$).[10,11,12]

MNPs have already been utilized in several biomedical applications [6,7,12–14]. To demonstrate how MNP structure and the resulting properties are intertwined, we can use a specific application to identify the parameters that tune crucial magnetic properties. In biosensing, for example, nanoparticles with higher saturation magnetization are preferred because they provide higher sensitivity and efficiency [2]. It has been demonstrated in several studies (vide infra) [15] that saturation magnetization increases linearly with size until it reaches the bulk value. While the correlation between magnetization and shape is not as direct, the effect of geometry on magnetic properties continues to be evaluated for biosensing applications [16,17]. A recent report pointed out the increased sensitivity of cubic MNPs for a biosensing platform owing to the increase in contact area for a cube in comparison to a sphere [18]. Composition also plays a significant role in influencing magnetic properties. However, due to concerns about the toxicity of the elements or compounds involved, the effect of the variation of composition has generally only been examined for ex

vivo applications; consequently, data related to applications involving biological contact reflect these limitations. For implantable biosensors such as glucose monitoring systems, biocompatibility has been a significant challenge. These concerns also exist for the various magnetic materials used in research and have frequently been addressed by encapsulating the MNP in an appropriate coating [19]. The nature of the coating is an important consideration in such shell-core MNP designs since the coating might enhance or significantly reduce the magnetic properties of the core based on the interaction between the ligand and the nanoparticle surface [7], the relative thickness of the shell, and the size of the nanoparticle being coated [20,21].

From this initial example, it is apparent that an understanding of the effectiveness of the various types of MNPs from a specific application-based perspective fails to provide the full picture of how to optimize an MNP system. For this reason, the bulk of the text that follows will focus on the influence of specific parameters on magnetic properties. Although we are aware that a combination of parameters might be involved in determining the effectiveness of a MNP for a specific application, for simplicity, we have listed tunable magnetic properties of fundamental importance for several applications in Table 1. These properties will be defined in the following section. We have also provided a brief list of published research focused on the key MNP parameters in Table 2. To maintain the practical utility of this review, we have focused on the following parameters that can be easily manipulated to tune the magnetic properties of the MNPs (Figure 1) using appropriate synthesis methods: (1) size; (2) shape; (3) composition; and (4) shell-core design. However, to provide context, the section that follows briefly outlines the fundamentals of nanomagnetism.

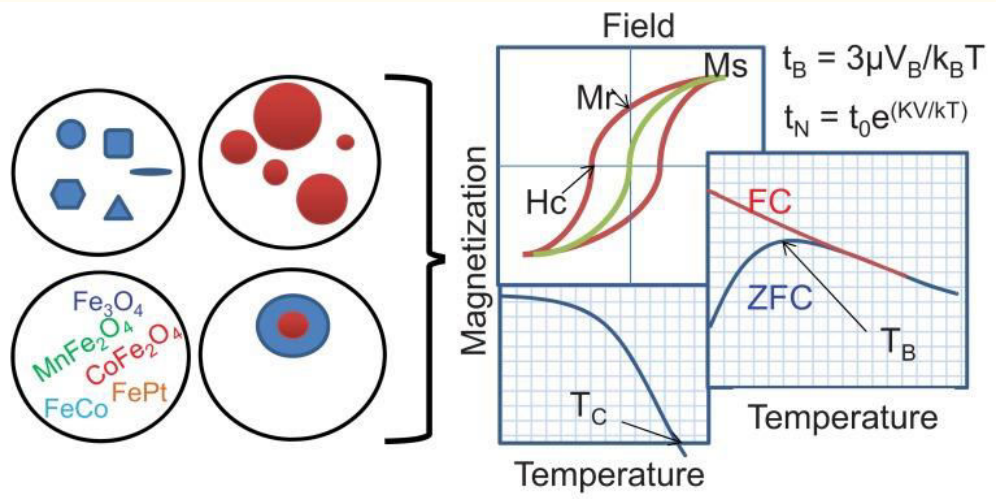


Figure 1

Effects of various parameters (e.g., shape, size, composition, architecture) on the magnetic properties of MNPs. (Abbreviations and magnetic property-based nomenclature has been defined and discussed in the following sections).

The design of MNPs with tailored properties depends on the fundamental concepts of nanomagnetism (i.e., magnetism observed in nanoparticles). A review of what produces magnetization, including the relationship between various extrinsic and intrinsic parameters, will enable us to better evaluate the underlying factors that influence magnetism at the nanoscale. Explanations about the role of atomic and molecular structure upon magnetization are readily available [55]. However, from a practical perspective, most of what we need to know to manipulate the effectiveness of these nanoscale magnets can be derived from prior experimental observations and an understanding of the role of MNP magnetic domain structure.

Based on the response of the intrinsic MNP magnetic dipole and the net magnetization in the presence and absence of an applied magnetic field, MNPs are typically classified as being either diamagnetic, paramagnetic, ferromagnetic, ferrimagnetic, and antiferromagnetic [56,57]. Figure 2 shows the net magnetic dipole arrangement for each of these types of magnetic materials. For diamagnetic materials in the absence of a magnetic field, magnetic dipoles are not present. However, upon application of a field, the material produces a magnetic dipole that is oriented opposite to that of the applied field; thus, a material that has strong diamagnetic character is repelled by a magnetic field. For paramagnetic materials, there exist magnetic dipoles as illustrated in Figure 2, but these dipoles are aligned only upon application of an external magnetic field. For the balance of the magnetic properties illustrated in Figure 2, the magnetization in the absence of an applied field reveals their fundamental character. Ferromagnetic materials have net magnetic dipole moments in the absence of an external magnetic field. In antiferromagnetic and ferrimagnetic

materials, the atomic level magnetic dipole moments are similar to those of ferromagnetic materials, however, adjacent dipole moments exist that are not oriented in parallel and effectively cancel or reduce, respectively, the impact of neighboring magnetic dipoles within the material in the absence of an applied field.

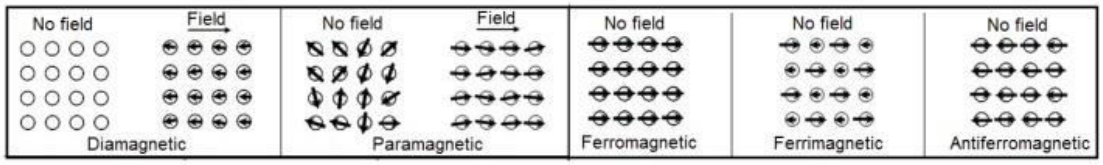


Figure 2

Magnetic dipoles and behavior in the presence and absence of an external magnetic field. Based on the alignment and response of magnetic dipoles, materials are classified as diamagnetic, paramagnetic, ferromagnetic, ferrimagnetic, antiferromagnetic.

Research in magnetic nanoparticles typically focuses on developing an optimal response for MNPs to an external magnetic field, and the majority of the published research has involved MNPs that are typically classified as either ferrimagnetic, ferromagnetic, or superparamagnetic particles (a special case of ferro- or ferri-magnetic particles). Below certain critical dimensions (that vary with the material parameters), MNPs exhibit magnetic responses reminiscent of those of paramagnetic materials, which is a zero average magnetic moment in the absence of an external field and a rapidly increasing (as compared to paramagnetic materials) magnetic moment under application of an external field in the direction of the field. This phenomenon, observed at temperatures above the so-called blocking temperature (see below), arises from the thermal fluctuations within the nanoparticles being comparable to or greater than the energy barrier for moment reversal, allowing rapid random flipping of the nanoparticle magnetic moments. In the case where the magnetization of the MNP over the measurement/observation interval is equal to zero in the absence of an external field, such nanoparticles are referred to as superparamagnetic. Superparamagnetism is especially important in applications such as drug delivery or MRI, where the nanoparticles exhibit no magnetic properties upon removal of the external field and therefore have no attraction for each other, eliminating the major driving force for aggregation. More importantly, superparamagnetic nanoparticles allow better control over the application of their magnetic properties because they provide a strong response to an external magnetic field.

For MNPs, the maximum magnetization possible is called the saturation magnetization, and it arises when all the magnetic dipoles are aligned in an external magnetic field. Figure 3 shows a typical magnetization curve for ferromagnetic or ferrimagnetic nanoparticles showing the characteristic positions on the curve associated with saturation magnetization (Ms, maximum induced magnetization), remanent magnetization (Mr, induced magnetization remaining after an applied field is removed), and coercivity (H, the intensity of an external coercive field needed to force the magnetization to zero). In the same figure, in contrast to the hysteresis observed in the case of ferromagnetic nanoparticles (red loop), the response of superparamagnetic nanoparticles to an external field also follows a sigmoidal curve but shows no hysteresis (green line). The response of paramagnetic (blue line) and diamagnetic (black line) nanoparticles is also shown in the schematic. The Ms shown in Figure 3 depends on temperature and is at a maximum at 0 K when the thermal vibrations (and thus randomization of aligned moments) are reduced.

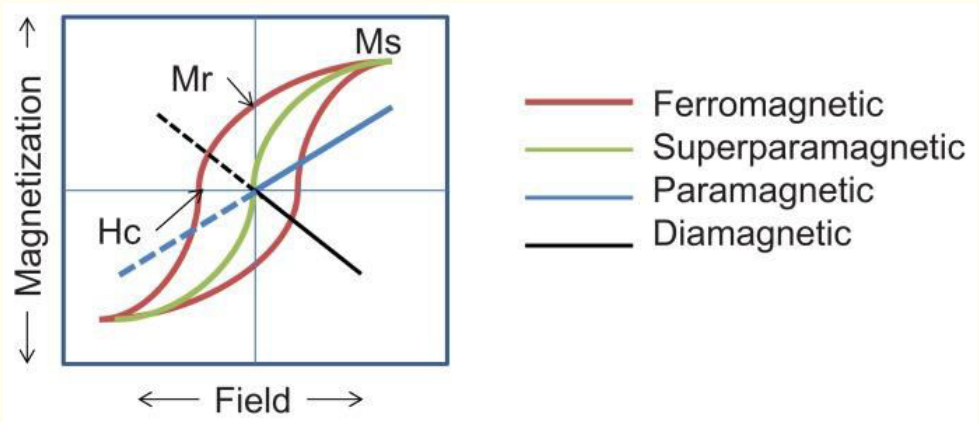


Figure 3

Magnetic behavior under the influence of an applied field, as further described in the text. The X-axis is the applied field (Oe), and the Y-axis is the magnetization of the sample as a function of field exposure (emu/g). Reproduced with permission from [6].

## IV. CONCLUSION

The magnetic nanoparticle is an important type of nanoparticle. It contains two parts, a magnetic material such as iron, nickel or cobalt, and a chemical component. The presence of a single magnetic nanoparticle is called a magnetic nanobead, and it has a size of 50–200 nm. Clusters of magnetic nanoparticles are a basic unit for further collaboration into magnetic nanochains. These nanoparticles are used in medical science, data storage, tissue engineering, magnetic imaging, and sensing of pollutants. From these magnetic nanoparticles, ferrites are used largely because of the spinel structure with high thermal stability, medium magnetization, chemical stability, and high surface area. [13,14,15]The merits of magnetic nanoparticles include: (1) greater efficiency; (2) easy separation of catalyst after removal of pollutant; (3) biodegradable, stable, and recyclable; (4) low cost and single-step reaction for synthesis; and (5) small size, high surface and magnetic properties. Different types of magnetic nanoparticles are reported such as oxide ferrites, ferrites with shells, metallic, metallic with shells. Fig. 7 shows the synthesis of ferrite nanoparticles by using two metal salt solutions. For the synthesis of these magnetic nanomaterials, generally three strategies are available: (1) physical method; (2) chemical method; and (3) microbial method. The major limitation of the physical method is to synthesize controlled size and morphology nanoparticles. Chemical coprecipitation, hydrothermal, sol gel, polyol, electrochemical, and vapor deposition methods are several strategies followed under the wet chemical preparation method. Wet deposition methods dominate over physical methods in terms of controlling particle size, but the use of toxic chemicals is a major limitation. In terms of an ecofriendly approach, microbial synthesis is used worldwide. Natural products of plants, agricultural waste, and microorganisms are used in synthesis. Better reproducibility, biocompatibility, scalability, and control of the particle size are attributes of the microbial synthesis method. These magnetic nanoparticles are largely used for the removal of pesticides, dyes, heavy metals, and organic and inorganic pollutant from contaminated water and soil by adsorption. From the literature survey, it was found that the adsorption phenomenon depends on electrostatic attraction, the surface area of the nanocatalyst, and the temperature and pH of the wastewater. For comparison, magnetic nanoparticles are synthesized by using both chemical and green methods. Eucalyptus extracts are used as a green source and iron sulfate as an iron source. Chemical synthesis is oxidation by using NaOH and high temperature to obtain $Fe^{2+}$ and $Fe^{3+}$ while green synthesis follow reduction means start with $Fe^{3+}$. HR-TEM pictures confirmed that green magnetic synthesis is formed by aggregates of nanoparticles of 10–30 nm. The biosynthesis of Ag@ $CoFe_2O_4$ with tulsi seeds (Ocimum sanctum) and garlic cloves (Allium sativum) gives the cubical-shaped Ag@ $CoFe_2O_4$ nanocomposite, which was confirmed by FE-SEM results. Cobalt ferrite (inverse spinel) has shown anisotropy with large magnetic saturation. Ag increases the antimicrobial properties of $CoFe_2O_4$ after doping of Ag in $CoFe_2O_4$. The fungus Monascus purpureus is used for the synthesis of spherical supermagnetic cobalt ferrite. By using different characterization techniques, the particle size is 6.50 nm. XRD pattern confirmed the single-phase crystalline structure. Spinel ferrite nanoparticles have also gained popularity among researchers due to the unique optical, magnetic, and electrical properties. [16,17,18]The general formula of spinels is $MFe_2O_4$ where M is a different type of metal. The spinel $Zn_xCo_{1-x}Fe_2O_4$ is synthesized by using curd as a green fuel than used for the study of the photocatalytic and antibacterial activity. The shape of the ferrite nanoparticle is spherical and the uniform distribution of particles and confirmed particle size in nm range are confirmed. For the analysis of bandgap, the DFT technique is used, which is similar to the practical values. It was concluded that the samples were visible active materials. The recombination rate of photogenerated electron-hole pairs reduces with enhancing zinc doping is analyzed in dropping of luminescence intensity of ferrite. To study the same application, part cubic spinel $ZnFe_2O_4$ is also synthesized by using Limonia acidissima juice with a particle size of 20 nm. EDS analysis confirmed the purity of the spinel ferrite nanoparticle. By using Juglans regia green husk extract,[19] the synthesis of $Fe_3O_4$/Au of size 6.08 ± 1.06 nm via the coprecipitation method was done. Using the TGA technique showed the weight loss of Juglans regia/iron oxide nanoparticle and core shell $Fe_3O_4$/Au are 88.03% and 81.87%, respectively. The last 6.16% of the weight loss is mainly due to the evaporation phenomenon of the gold shell.[20]

## REFERENCES

1. Tadic, Marin; Kralj, Slavko; Jagodic, Marko; Hanzel, Darko; Makovec, Darko (December 2014). "Magnetic properties of novel superparamagnetic iron oxide nanoclusters and their peculiarity under annealing treatment". Applied Surface Science. 322: 255–264. Bibcode:2014ApSS..322..255T. doi:10.1016/j.apsusc.2014.09.181.
2. ^ Magnetic Nanomaterials, Editors: S H Bossmann, H Wang, Royal Society of Chemistry, Cambridge 2017, https://pubs.rsc.org/en/content/ebook/978-1-78801-037-5

3. ^ [a] [b] Kralj, Slavko; Makovec, Darko (27 October 2015). "Magnetic Assembly of Superparamagnetic Iron Oxide Nanoparticle Clusters into Nanochains and Nanobundles". ACS Nano. 9 (10): 9700–9707. doi:10.1021/acsnano.5b02328. PMID 26394039.
4. ^ A.-H. Lu; W. Schmidt; N. Matoussevitch; H. Bönnemann; B. Spliethoff; B. Tesche; E. Bill; W. Kiefer; F. Schüth (August 2004). "Nanoengineering of a Magnetically Separable Hydrogenation Catalyst". Angewandte Chemie International Edition. 43 (33): 4303–4306. doi:10.1002/anie.200454222. PMID 15368378.
5. ^ A. K. Gupta; M. Gupta (June 2005). "Synthesis and surface engineering of iron oxide nanoparticles for biomedical applications". Biomaterials. 26 (18): 3995–4021. doi:10.1016/j.biomaterials.2004.10.012. PMID 15626447.
6. ^ Ramaswamy, B; Kulkarni, SD; Villar, PS; Smith, RS; Eberly, C; Araneda, RC; Depireux, DA; Shapiro, B (24 June 2015). "Movement of magnetic nanoparticles in brain tissue: mechanisms and safety". Nanomedicine: Nanotechnology, Biology and Medicine. 11 (7): 1821–9. doi:10.1016/j.nano.2015.06.003. PMC 4586396. PMID 26115639.
7. ^ He, Le; Wang, Mingsheng; Ge, Jianping; Yin, Yadong (18 September 2012). "Magnetic Assembly Route to Colloidal Responsive Photonic Nanostructures". Accounts of Chemical Research. 45 (9): 1431–1440. doi:10.1021/ar200276t. PMID 22578015.
8. ^ Kavre, Ivna; Kostevc, Gregor; Kralj, Slavko; Vilfan, Andrej; Babič, Dušan (13 August 2014). "Fabrication of magneto-responsive microgears based on magnetic nanoparticle embedded PDMS". RSC Advances. 4 (72): 38316–38322. Bibcode:2014RSCAd...438316K. doi:10.1039/C4RA05602G.
9. ^ Mornet, S.; Vasseur, S.; Grasset, F.; Veverka, P.; Goglio, G.; Demourgues, A.; Portier, J.; Pollert, E.; Duguet, E. (July 2006). "Magnetic nanoparticle design for medical applications". Progress in Solid State Chemistry. 34 (2–4): 237–247. doi:10.1016/j.progsolidstchem.2005.11.010.
10. ^ B. Gleich; J. Weizenecker (2005). "Tomographic imaging using the nonlinear response of magnetic particles". Nature. 435 (7046): 1214–1217. Bibcode:2005Natur.435.1214G. doi:10.1038/nature03808. PMID 15988521. S2CID 4393678.
11. ^ Hyeon, Taeghwan (3 April 2003). "Chemical synthesis of magnetic nanoparticles". Chemical Communications (8): 927–934. doi:10.1039/B207789B. PMID 12744306. S2CID 27657072.
12. ^ [a] [b] Natalie A. Frey and Shouheng Sun Magnetic Nanoparticle for Information Storage Applications
13. ^ Elliott, Daniel W.; Zhang, Wei-xian (December 2001). "Field Assessment of Nanoscale Bimetallic Particles for Groundwater Treatment". Environmental Science & Technology. 35 (24): 4922–4926. Bibcode:2001EnST...35.4922E. doi:10.1021/es0108584. PMID 11775172.
14. ^ J. Philip; Shima.P.D. B. Raj (2006). "Nanofluid with tunable thermal properties". Applied Physics Letters. 92 (4): 043108. Bibcode:2008ApPhL..92d3108P. doi:10.1063/1.2838304.
15. ^ Chaudhary, V.; Wang, Z.; Ray, A.; Sridhar, I.; Ramanujan, R. V. (2017). "Self pumping magnetic cooling". Journal of Physics D: Applied Physics. 50 (3): 03LT03. Bibcode:2017JPhD...50cLT03C. doi:10.1088/1361-6463/aa4f92.
16. ^ J.Philip; T.J.Kumar; P.Kalyanasundaram; B.Raj (2003). "Tunable Optical Filter". Measurement Science and Technology. 14 (8): 1289–1294. Bibcode:2003MeScT..14.1289P. doi:10.1088/0957-0233/14/8/314. S2CID 250923543.
17. ^ Mahendran, V. (2012). "Nanofluid based opticalsensor for rapid visual inspection of defects in ferromagnetic materials". Appl. Phys. Lett. 100 (7): 073104. Bibcode:2012ApPhL.100g3104M. doi:10.1063/1.3684969.
18. ^ Chaudhary, V.; Ramanujan, R. V. (11 October 2016). "Magnetocaloric Properties of Fe-Ni-Cr Nanoparticles for Active Cooling". Scientific Reports. 6 (1): 35156. Bibcode:2016NatSR...635156C. doi:10.1038/srep35156. PMC 5057077. PMID 27725754.
19. ^ Chaudhary, V.; Chen, X.; Ramanujan, R.V. (February 2019). "Iron and manganese based magnetocaloric materials for near room temperature thermal management". Progress in Materials Science. 100: 64–98. doi:10.1016/j.pmatsci.2018.09.005. hdl:10356/142917. S2CID 139870597.
20. ^ Philip, V. Mahendran; Felicia, Leona J. (2013). "A Simple, In-Expensive and Ultrasensitive Magnetic Nanofluid Based Sensor for Detection of Cations, Ethanol and Ammonia". Journal of Nanofluids. 2 (2): 112–119. doi:10.1166/jon.2013.1050.

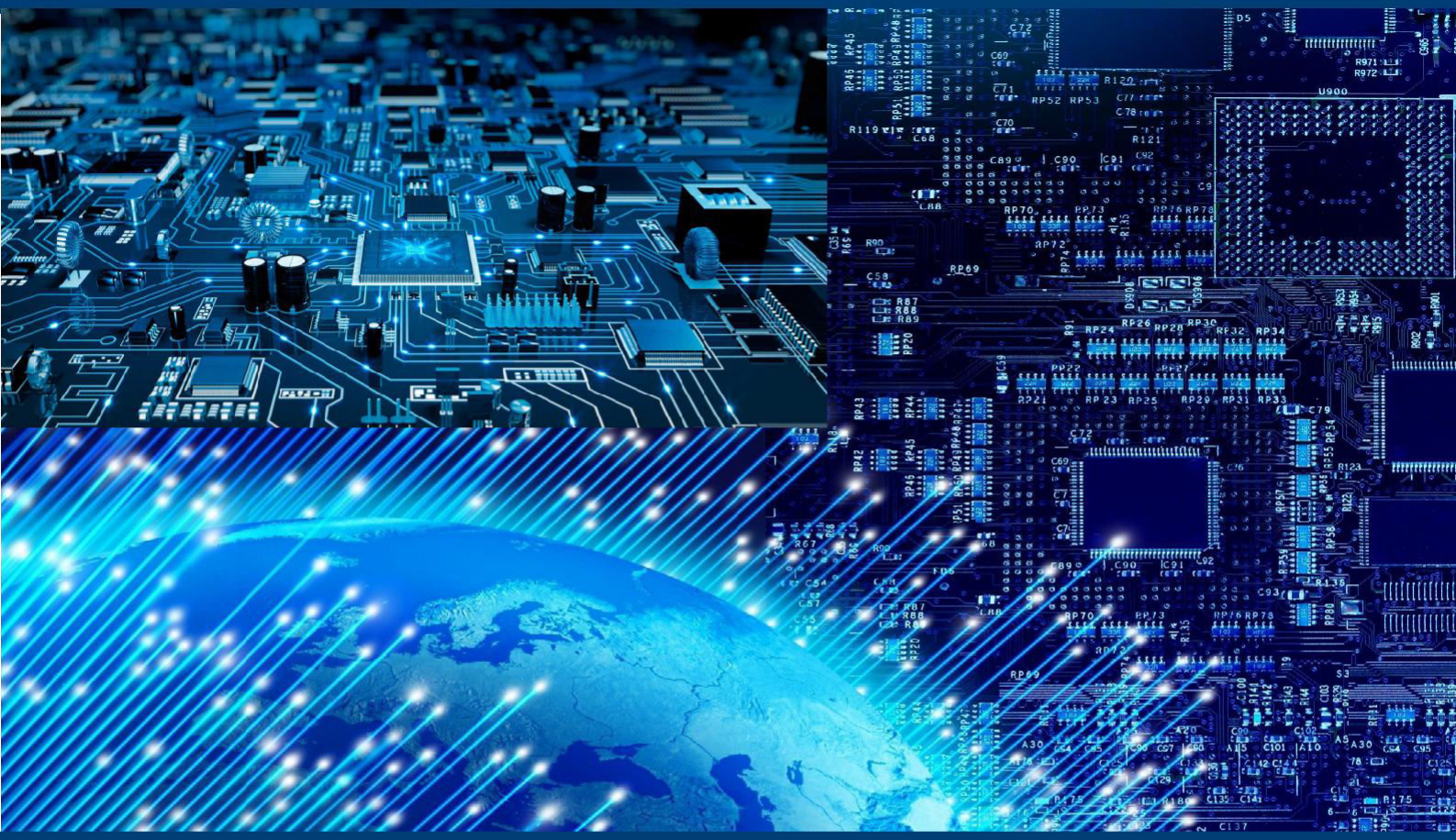


# International Journal of Advanced Research in Arts, Science, Engineering & Management (IJARASEM)



| Mobile No: +91-9940572462 | Whatsapp: +91-9940572462 | ijarasem@gmail.com |